AD-A139 809 REPEATABILITY OF MIXED-MODE ADHESIVE DEBONDING(U) 1/1
NATIONAL AERONAUTICS AND SPACE ADMINISTRATION HAMPTON
VA LANG.. R A EVERETT ET AL. FEB 84 NASA-TM-85753
UNCLASSIFIED USAAVSCOM-TR-84-B-1 F/G 13/8 NL

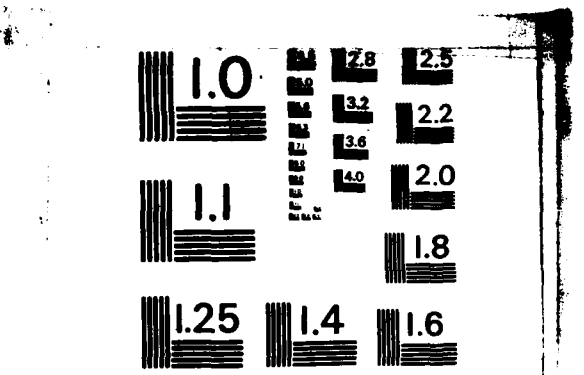

NASA Technical Memorandum 85753

USAAVSCOM Technical Report 84-B-1

REPEATABILITY OF MIXED-MODE ADHESIVE DEBONDING

R. A. Everett, Jr. and W. S. Johnson

February 1984

NASA
National Aeronautics and
Space Administration
Langley Research Center
Hampton, Virginia 23665

REPEATABILITY OF MIXED-MODE ADHESIVE DEBONDING

R. A. Everett, Jr.* and W. S. Johnson
NASA Langley Research Center
Hampton, Virginia 23665

SUMMARY

An experimental study was undertaken to assess the repeatability of debond growth rates in adhesively bonded joints subjected to constant-amplitude cyclic loading. This was done by comparing debond growth rates from two sets of cracked-lap-shear specimens that were fabricated by two different manufacturers and tested in different laboratories. The fabrication method and testing procedure were identical for both sets of specimens. The specimens consisted of aluminum adherends bonded with FM-73 adhesive. Critical values of strain-energy-release rate were also determined from specimens that were monotonically loaded to failure. The test results showed that the debond growth rates for the two sets of specimens were within a scatter band which is similar to that observed in fatigue crack growth in metals. Cyclic debonding occurred at strain-energy-release rates that were more than an order of magnitude less than the critical strain-energy-release rate in static tests.

*Structures Laboratory, U.S. Army Research and Technology Laboratories (AVSCOM), NASA Langley Research Center, Hampton, Virginia 23665.

INTRODUCTION

One of the factors that has delayed the widespread use of adhesively bonded structures, especially in primary aircraft structures, is the question of joint reliability. In the last few years more aircraft manufacturers have started using adhesively bonded joints in primary structures partly because of proven fabrication methods. This is especially true in aluminum structures where the phosphoric acid anodize cleaning procedure [1] has been shown to produce reliable bonded joints, even in adverse environments. Even though reliable fabrication methods have been developed, there will always be variations in these methods from manufacturer to manufacturer, as well as differences that arise from other sources such as material variability. If the service life of bonded structures is going to be predicted with any satisfactory accuracy using analytical techniques such as fracture mechanics [2], the repeatability of experimental data used in these techniques must be within an acceptable scatter band. Since this repeatability will be affected by variations in fabrication methods as well as material variability, the effects of these factors on repeatability must be assessed before confidence can be established in designing adhesively bonded structures. The main purpose of the study reported herein is to obtain data on adhesive bond repeatability by comparing debond growth data from specimens made by two different manufacturers and tested in different laboratories.

The Air Force has sponsored several research programs using fracture mechanics as the analytical tool in predicting the service life of bonded structures [2,3,4,5]. A large debond growth rate data base was established in the Integrated Methodology for Adhesive Bonded Joint Life Prediction Program [5]. For economics and convenience, this data base was chosen to compare data. The Integrated Methodology program [5] used the information generated under the

previous programs [2,3,4] to develop a "logical and internally consistent method for predicting the service life of bonded joints." The main emphasis of the Integrated Methodology program was in the analytical prediction of service life. To demonstrate the predictive capabilities of this method, a joint called the structural lap joint was designed and tested to simulate the fatigue behavior of a production joint on the PABST fuselage [6] called a circumferential bonded splice joint. To predict the service life of the structural lap joint, fracture mechanics parameters such as strain-energy-release rate versus debond growth rate data were determined from fatigue tests on the cracked-lap-shear specimen.

In the test program described in this paper, cracked-lap-shear specimens were manufactured and tested in an identical manner as the specimens used in the Integrated Methodology program [5]. Constant-amplitude fatigue tests were run at several load levels and the debond growth rates were compared with the test results from the Integrated Methodolgy program. The debond growth rates were correlated using strain-energy-release rates that were calculated using a finite-element analysis. Critical values of strain-energy-release rate were also determined for tests where the specimen was loaded monotonically to failure.

SPECIMEN GEOMETRY AND MANUFACTURE

The cracked-lap-shear specimens used in this study were identical in geometry to the specimens used in the Integrated Methodology program [5]. The two specimen configurations, CLS1 and CLS2, are shown in Fig. 1. The different cross-sections were intended to provide a different mix of mode I and mode II strain-energy-release rates. The idea of using a side groove and the basic specimen geometry was suggested by Brussat, Chiu, and Mostovoy [2].

The presence of the grooves causes more load to be transferred across the bond for a given stress level in the adherend, thus reducing adherend fatigue problems.

The specimens used in this program were manufactured the same way as the Integrated Methodology program's [5] specimens. The 7075-T6 adherends were cleaned using the BAC-5555 (Boeing Aircraft Company) phosphoric acid anodize process [1] and then bonded together with FM-73* (American Cyanamid Company) adhesive using the manufacturer's recommended cure cycle of time, temperature, and pressure. The FM-73 was used in the FM-73M sheet form of 0.38 mm thickness.

Two 86 mm by 95 mm plates, 6.35 mm and 19.05 mm thick, were bonded in an autoclave and then the individual specimens were cut from the bonded plates. The autoclave applies uniform pressure, but not necessarily uniform displacements. The adhesives were freer to flow at the edges than in the center of the plate, resulting in a thicker bondline in the center. A typical variation of the bondline thickness along the specimen length is shown in Fig. 2.

TESTING PROCEDURE

Constant-amplitude fatigue tests were run in a closed-loop servo-hydraulic test machine at frequencies of 3 and 10 Hz. All tests were run at a stress ratio of 0.10. The debond growth data were measured over a region of 76 to 322 mm from the lap end, thus avoiding the thin bondlines in the end regions as shown in Fig. 2. Tests were conducted at three or more constant-amplitude load levels for each specimen to get several values of debond growth rate (da/dN).

---

*The use of trade names in this paper does not constitute endorsement, either expressed or implied, by the National Aeronautics and Space Administration.

For both specimen configurations, two specimens were run at each test frequency. Figure 3 shows typical debond data for different load levels. The load levels and the debond length over which debond growth rates were measured were the same as used in the Integrated Methodolgy program [5] and are given in Table 1. At the conclusion of each debond test, each specimen was loaded monotonically to failure to determine a critical failure load, which was used to calculate a critical strain-energy-release rate.

Two techniques were used to monitor the debond growth. The first method used a small, portable, ultrasonic device with a hand-held transducer to locate the debond front. The second method involved locating the debond front visually by using a seven-power monocular. For each technique, the number of cycles required to advance the debond front an additional 0.254 mm was recorded. The majority of the data were taken using the visual technique. The ultrasonic technique was not used after the first two tests because of difficulties encountered in adjusting the various parameters needed to achieve a repeatable ultrasonic signal that could be identified as representing the debond front.

Loads were applied to each end of the specimens through a double-clevis arrangement, as shown in Fig. 4, allowing the specimen to rotate freely. Each specimen was mounted in the clevis so that the centerline through the thickness of both ends of the specimen was coincident with the centerline of the clevis. This procedure for mounting the specimens in the clevis and the design of the double-clevis arrangement were identical to that used in the Integrated Methodology program [5].

FINITE-ELEMENT ANALYSIS

Studies of debond propagation in adhesively bonded joints have shown that the strain-energy-release rate is a useful tool for correlating debond

propagation rates [2,4,5]. In this study a nonlinear geometric analysis using a two-dimensional finite-element program called GAMNAS [7] was used to calculate the strain-energy-release rate for each test condition. A nonlinear geometric analysis is needed to account for the large rotations that often occur in cracked-lap-shear specimens [7]. For the two-dimensional analysis done in this study, the plane-strain condition was used. The strain-energy-release rates were computed for the maximum load in the fatigue cycle using a virtual crack-closure technique. The details of this procedure are given in Ref 8. The material properties used in the analysis are given in Table 2.

For this analysis, the cracked-lap-shear specimen was modeled using a finite-element mesh which typically contained about 2300 isoparametric four-node elements and about 4800 degrees of freedom. A sketch of the mesh, along with the accompanying boundary conditions, is shown in Fig. 5. A single fixed node at both ends of the specimen was chosen as the boundary condition to simulate the loading conditions, as shown in Fig. 5. The double-clevis loading arrangement was designed so that the inner loading pin carried through the thickness of the specimen, while the outer clevis pin was parallel to the bondline. Hence, the rotations expected due to specimen eccentricity occurred mostly at the outer pins. Since the inner pins were not clamped, a tight fit was not achieved; thus, some relaxation of the moments would be expected to occur at these inner pins. Such boundary conditions are not suitable for theoretical modeling and may produce errors in the calculated strain-energy-release rates.

To account for the effect of the side groove in the specimen, a method similar to the equivalent or transformed cross-sectional area technique found in strength of materials [9] was used. Using this technique, the cross-section configuration was converted to a single-width configuration by scaling the

modulus of area B in Fig. 5 by the ratio of the full specimen width to the bondline width, i.e., $E_B = E_A(25/5)$. The material in the side groove adjacent to the adhesive, shown as area A in Fig. 5, was left as aluminum. Both the aluminum and the equivalent modulus material were modeled using six to eight finite-element layers. The adhesive was modeled using five layers of elements. This allowed the debond to be modeled between the first and second adhesive element layers adjacent to the strap adherend, as shown in Fig. 5. This was the general location of the adhesive debonds observed in the current study as well as that observed in other CLS tests [10].

In previous studies with the cracked-lap-shear specimen, the strain-energy-release rates were often found to be independent of the debond length [7,10]. However, with the specimen configurations used in this study G_T varied with the debond length, as shown in Fig. 6. As stated previously, the adhesive thickness varied along the debond length for each specimen. An analysis on the effect of adhesive thickness on G in the CLS1 specimen showed about 1 percent variation in G_T, about 15 percent in G_I, and about 4 percent in G_{II}. In geometrically linear systems, G is directly proportional to the square of the applied load (shown to be within 1 percent in Ref 10). In the present study, G varied by as much as 15 percent with the square of the applied load. Therefore, considering the variation of G with the previously mentioned parameters, the G for each test condition in this study was computed based on the appropriate adhesive thickness, debond length, and applied load.

RESULTS AND DISCUSSION

Debond growth rates for the tests conducted in this study and the growth rates determined from the Integrated Methodology program [5] are shown in Figs. 7 and 8 for the CLS1 and CLS2 specimens, respectively. Data from the

tests at 3 and 10 Hz are included. These data are also given in Table 1 where the debond growth rates are given for each load level and for the debond lengths over which the growth rates were determined.

The growth rates for the CLS1 specimens from the Integrated Methodology tests are consistently faster than the growth rates from the present study for the same test frequency. The Integrated Methodology data show that the growth rates are higher at 10 Hz than at 3 Hz, but the current data show no consistent effect of test frequency on growth rate.

The results for the CLS2 specimens are somewhat reversed from those found for the CLS1 specimens . The growth rates for the CLS2 specimens from the tests of the present study are generally faster than the Integrated Methodology growth rates. No consistent trend is seen in the growth rates as affected by test frequency. Because of the small number of test specimens used in both studies, no significant statistical trends could be drawn from these data. Generally, the growth rates varied by a factor of 2 to 7, which is similar to that observed in fatigue crack growth in metals [11]. Hence, the scatter in cyclic debond data should not be a major problem in using the data in design applications.

Since the CLS1 and CLS2 specimens have different ratios of G_I/G_{II} (approximately 0.24 and 0.10, respectively), an effort was made in the current study to determine if G_I, G_{II}, or G_T dominates the cyclic debonding process. To do this, the measured debond rates were correlated with each of the strain-energy-release rate measures by fitting a relationship of the form

$$\frac{da}{dN} = c(G)^n \tag{1}$$

to the data. The equation was first fit to the data for each type of specimen to see if the form of the relationship was appropriate. The values of c and

n, as well as the sum of errors, Σr^2, are given in Table 3 for each of the G measures. With the exception of the fit of G_I to the CLS2 data, Eq (1) seems to provide a good fit to the data and therefore is a good choice for trying to correlate the data for the two specimen configurations. The G_T measure appears to provide the best overall fit to the data for each specimen type, which agrees with earlier work of the authors [10]. However, no single equation in G_I, G_{II}, or G_T correlated the debond growth rates for both specimen configurations. In fact, as shown in Fig. 9, at all values of G_T the debond rates for the CLS2 specimens are two orders of magnitude faster than for the CLS1 specimen. If the strain-energy-release rate due to the peel separation (G_I) was the dominating factor as stated by previous studies [12,13,14,15], the CLS1 specimen should have the faster debond rate for a given G_T.

The reason for these large differences are unexplained, but may be related to the partly undefinable boundary conditions of the double-clevis end conditions. An attempt to verify the analytical strain-energy-release rate experimentally through compliance calibration measurements failed because of the variable restraint conditions in the clevis loading system. The pin bending and bearing flexibilities in the clevises represented approximately 60 percent of the total system displacements. Because of these difficulties, caution should be used when the double-clevis setup is used for pin loading.

The results of the specimens loaded monotonically to failure are given in Figs. 10 and 11 for the CLS1 and CLS2 specimens, respectively. A comparison of the fatigue and static results given in these figures shows that cyclic debonding occurred at strain-energy-release rates more than an order of magnitude below the static values.

CONCLUSIONS

An experimental study was undertaken to assess the repeatability of debond growth rates in adhesively bonded joints subjected to constant-amplitude cyclic loading. This was done by comparing debond growth rates from two sets of cracked-lap-shear specimens that were fabricated by two different manufacturers and tested in different laboratories. The fabrication method and the testing procedure were identical for both sets of specimens. The specimens consisted of aluminum adherend bonded with FM-73 adhesive. Critical values of strain-energy-release rate were determined from specimens that were monotonically loaded to failure. A finite-element analysis was conducted to compute the strain-energy-release rates which were used to correlate the debond growth data. The present study led to the following conclusions:

1. Debond growth rates for the two sets of specimens varied by a factor of 2 to 7, which is similar to that observed in fatigue crack growth in metals.

2. Cyclic debonding occurred at strain-energy-release rates more than an order of magnitude below the critical values.

3. Strain-energy-release rate did not correlate debond growth rates for the two specimen configurations.

REFERENCES

[1] "Preparation of Aluminum Surfaces for Structural Adhesives Bonding (Phosphoric Acid Anodizing)," ASTM Standard D3933-80, American Society for Testing and Materials, Philadelphia, PA.

[2] Brussat, T. R., Chiu, S. T., and Mostovoy, S., "Fracture Mechanics for Structural Adhesive Bonds--Final Report," AFML-TR-77-163, Air Force Materials Laboratory, 1977.

[3] Renton, W. J., "Structural Properties of Adhesives," Volume 1, AFML-TR-78-127, Air Force Materials Laboratory, 1978.

[4] Romanko, J. and Knauss, W. G., "Fatigue Behavior of Adhesively Bonded Joints," Volume 1, AFWAL-TR-80-4037, Air Force Wright Aeronautical Laboratories, 1980.

[5] Romanko, J., Liechti, K. M., and Knauss, W. G., "Integrated Methodology for Adhesive Bonded Joint Life Predictions," AFWAL-TR-82-4139, Air Force Wright Aeronautical Laboratories, 1982.

[6] "Primary Adhesively Bonded Structure Technology (PABST)--Phase II: Detail Design," AFFDL-TR-135, Air Force Flight Dynamics Laboratory, 1977.

[7] Dattaguru, B., Everett, R. A., Jr., Whitcomb, J. D., and Johnson, W. S., "Geometrically-Nonlinear Analysis of Adhesively Bonded Joints," NASA TM-84562, National Aeronautics and Space Administration, September 1982.

[8] Rybicki, E. F. and Kanninen, M. F., "A Finite Element Calculation of Stress Intensity Factors by a Modified Crack Closure Integral," Engineering Fracture Mechanics, vol. 9, no. 4, 1977, pp. 931-938.

[9] Popov, E. P., Mechanics of Materials, Prentice-Hall, Inc., New Jersey, 1976, pp. 144-149.

[10] Mall, S., Johnson, W. S., and Everett, R. A., Jr., "Cyclic Debonding of Adhesively Bonded Composites," NASA TM-84577, National Aeronautics and Space Administration, November 1982.

[11] Damage Tolerant Design Handbook, Battelle Metals and Ceramics Information Center, Columbus, OH, 1975.

[12] Hart-Smith, L. J., "Analysis and Design of Advanced Composite Bonded Joints," NASA CR-2218, National Aeronautics and Space Administration, 1973.

[13] Smith, C. S. and Patterson, D., "Design of Structural Connections in GRP Ship and Boat Hulls," Designing with Fiber Reinforcing Materials, Institute of Mechanical Engineers Conference Publications 1977-79, 1977.

[14] Ishai, O. and Girshengorn, T., "Strength of Bonded Aluminum-CFRP Single-Lap Joints," Adhesives Age, vol. 21, no. 7, July 1978, pp. 25-30.

[15] Everett, R. A., Jr., "The Role of Peel Stresses in Cyclic Debonding," Adhesives Age, vol. 26, no. 5, May 1983, pp. 24-29.

TABLE 1--Debond growth data.

Specimen Configuration	[a]ΔP, kN	[b]a_i to [c]a_f, mm	da/dN, m/cycle			
			3 Hz		10 Hz	
			CLS1-2	CLS1-3	CLS1-5	CLS1-7
CLS1	17.79	76 → 112	2.8×10^{-8}	2.1	3.3	5.8
	22.24	114 → 155	11.1	11.2	15.0	18.0
	26.69	155 → 203	46.7	33.8	26.7	40.1
	31.14	203 → 239	93.2	112.0	77.5	69.9
	35.58	241 → 279	247.0	211.0	130.0	...
	40.03	279 → 323	851.0	605.0	452.0	...
			CLS2-5	CLS2-7	CLS2-6	CLS2-3
CLS2	8.90	79 → 119	9.7×10^{-8}	28.7	9.1	37.1
	11.12	127 → 158	109.0	...	44.2	106.0
	13.34	160 → 203	442.0	298.0	340.0	526.0
	15.57	203 → 267	6320.0	1200.0	3780.0	5111.0
	17.79	267 → 318	...	...	6630.0	30000.0

[a]Alternating load in fatigue cycle.

[b]Beginning of debond length measurement.

[c]End of debond length measurement.

TABLE 2--Material properties for finite-element analysis.

	Modulus, GPa		Poisson's Ratio
	E	G	ν
Aluminum	72.4	27.2	0.33
FM-73 (American Cyanamid Company)	1.64	0.59	0.40

TABLE 3--Regression analysis results.

		G_I	G_{II}	G_T
CLS1	c	8.13×10^{-14}	3.63×10^{-15}	1.67×10^{-15}
	n	2.86	2.71	2.74
	Σr^2	0.30	0.32	0.31
CLS2	c	2.63×10^{-7}	1.29×10^{-15}	3.16×10^{-16}
	n	1.01	3.54	3.74
	Σr^2	16.2	2.12	1.79

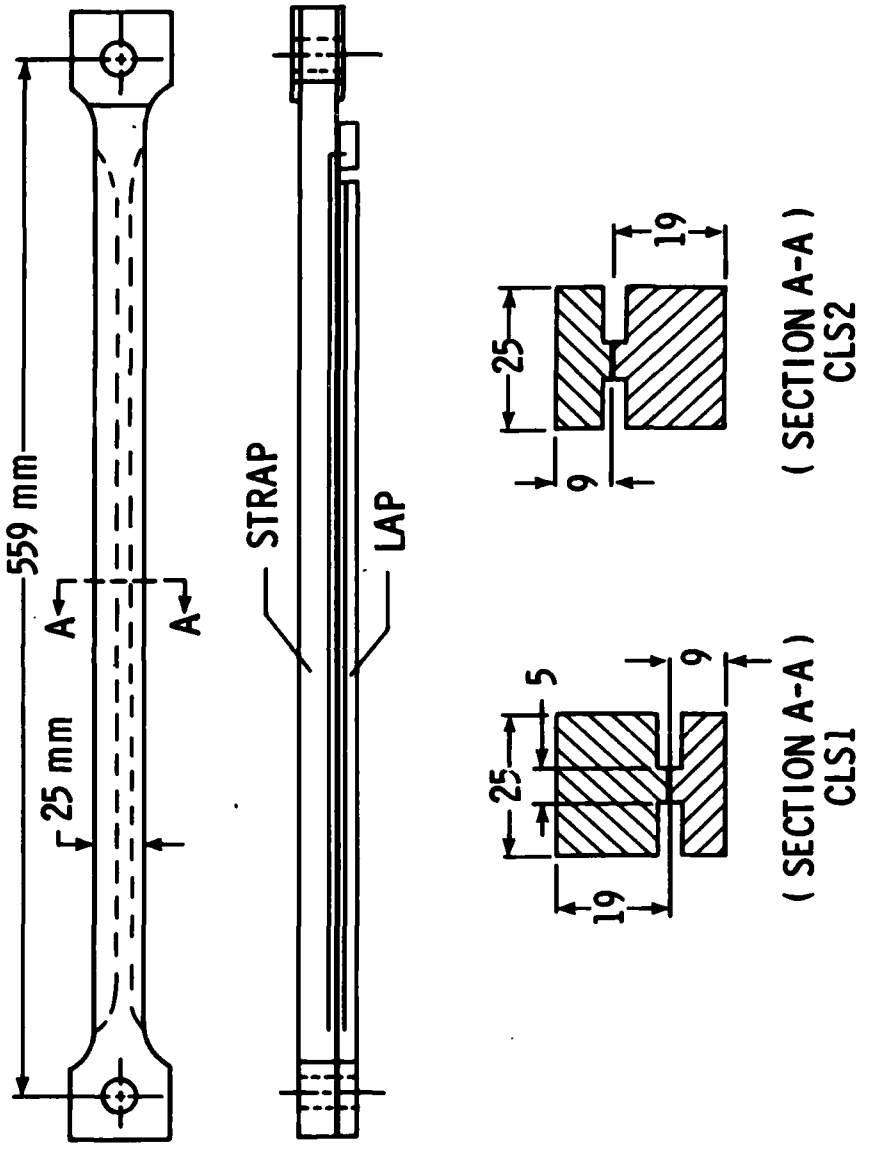

Fig. 1--Cracked-lap-shear specimen configuration.

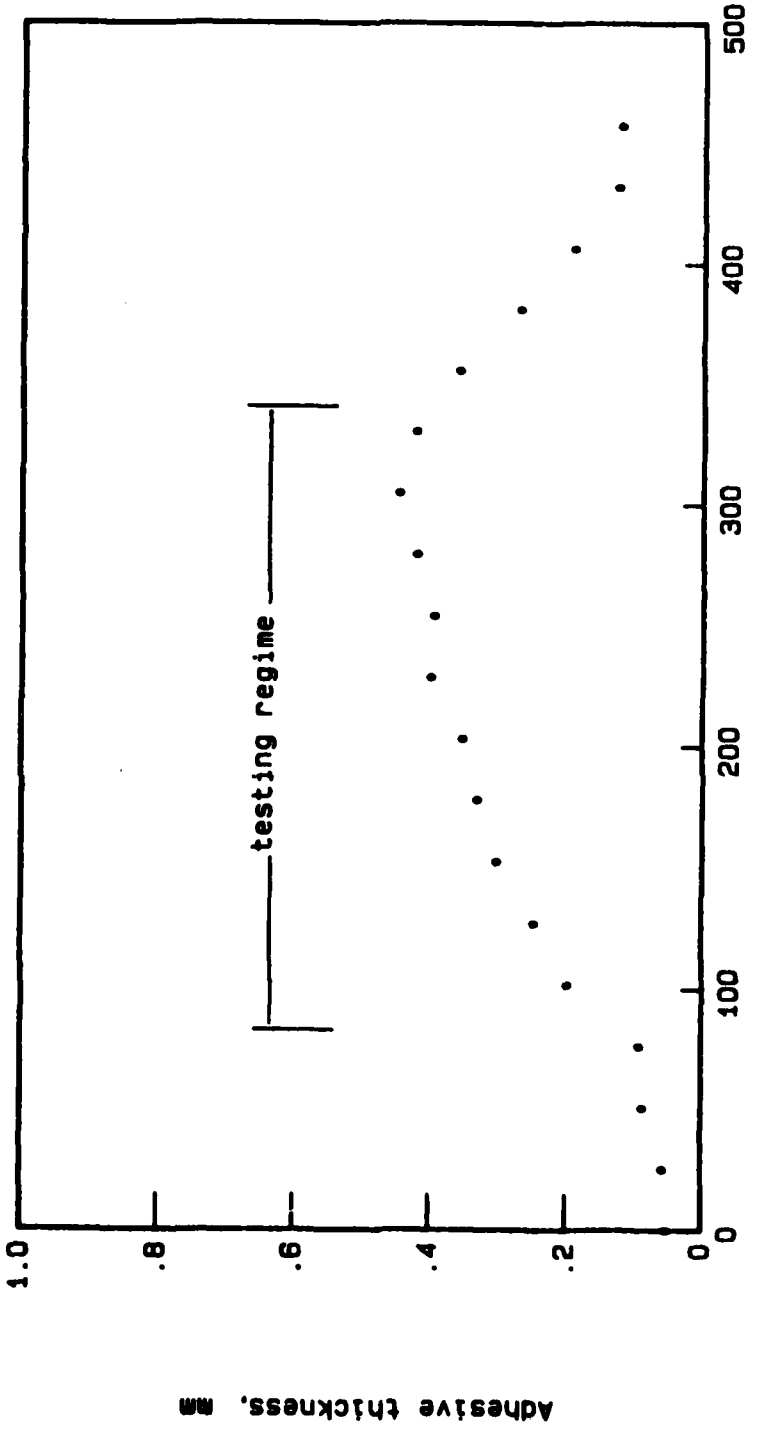

Fig. 2--Typical variation of adhesive thickness with lap length.

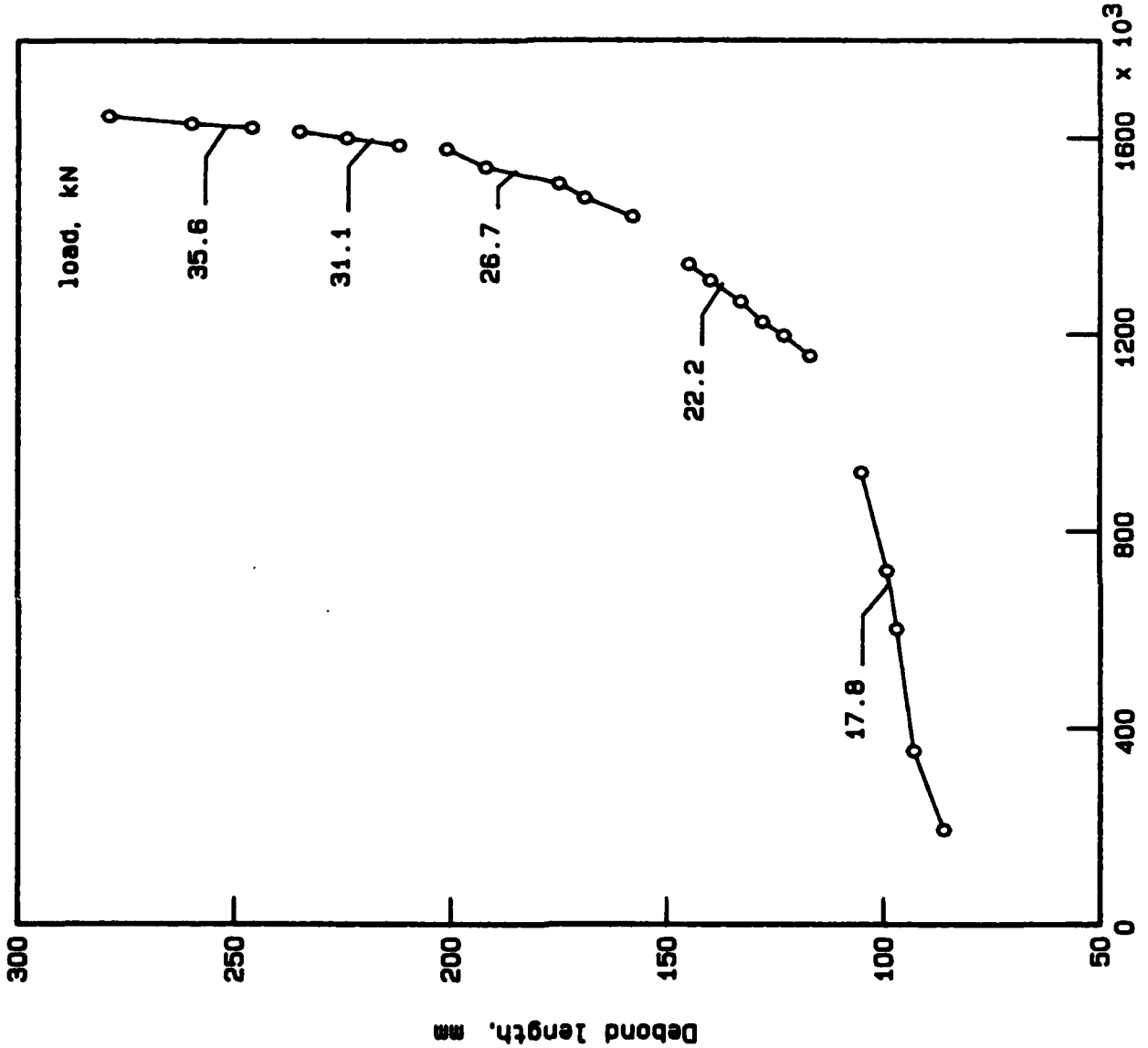

Fig. 3--Typical debond growth data.

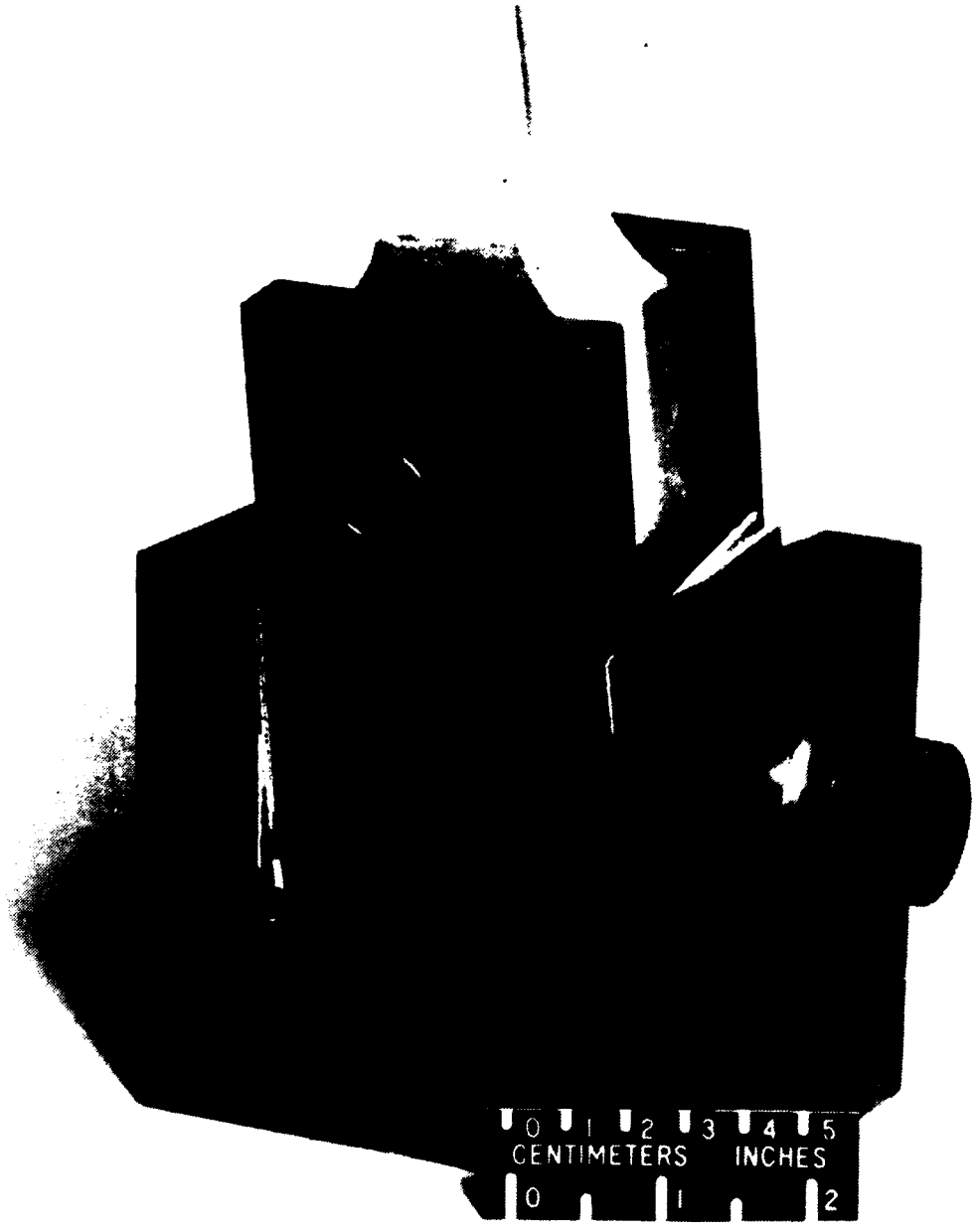

Fig. 4--Double-clevis pin-loading arrangement.

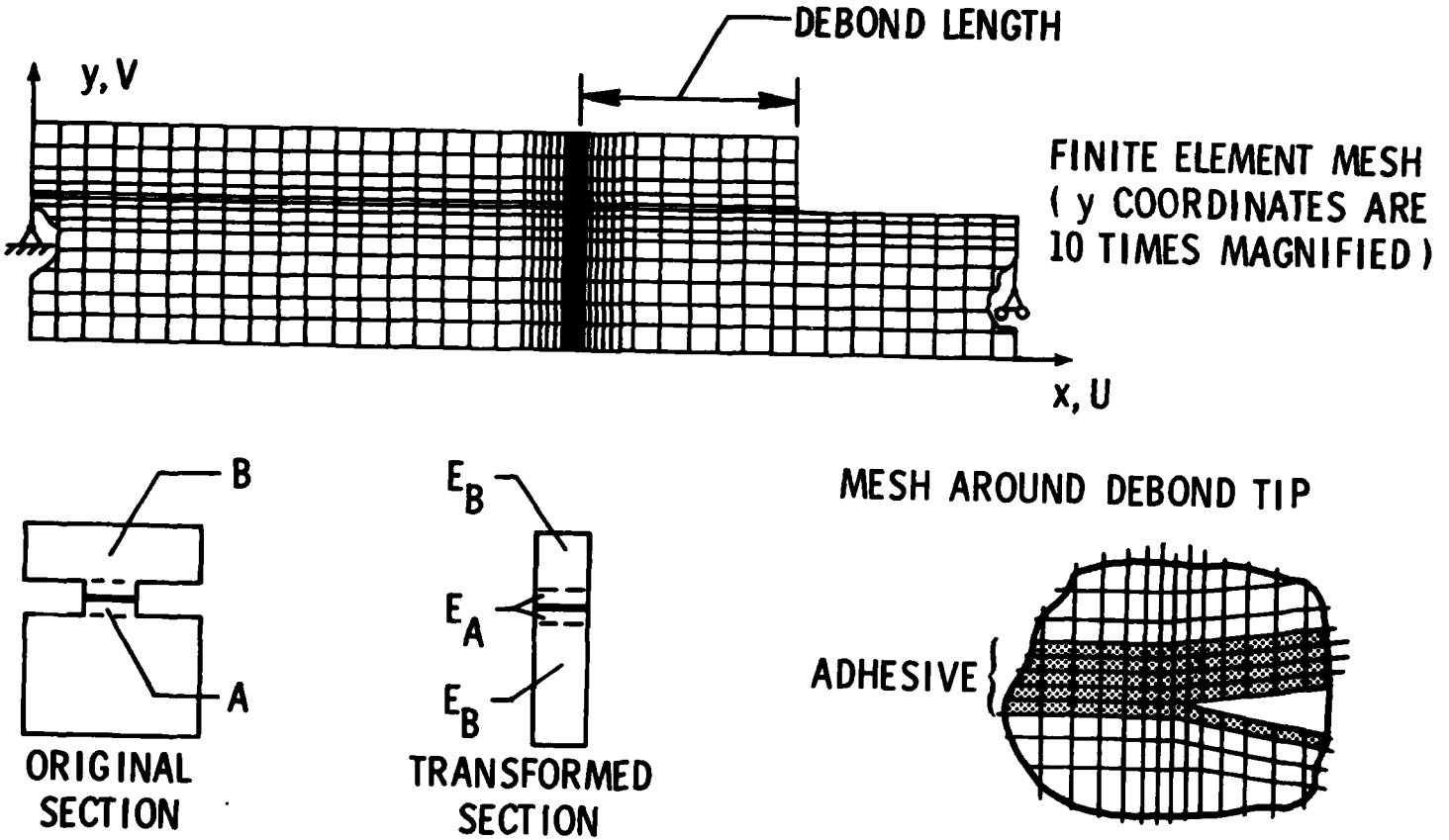

Fig. 5--Typical finite-element model.

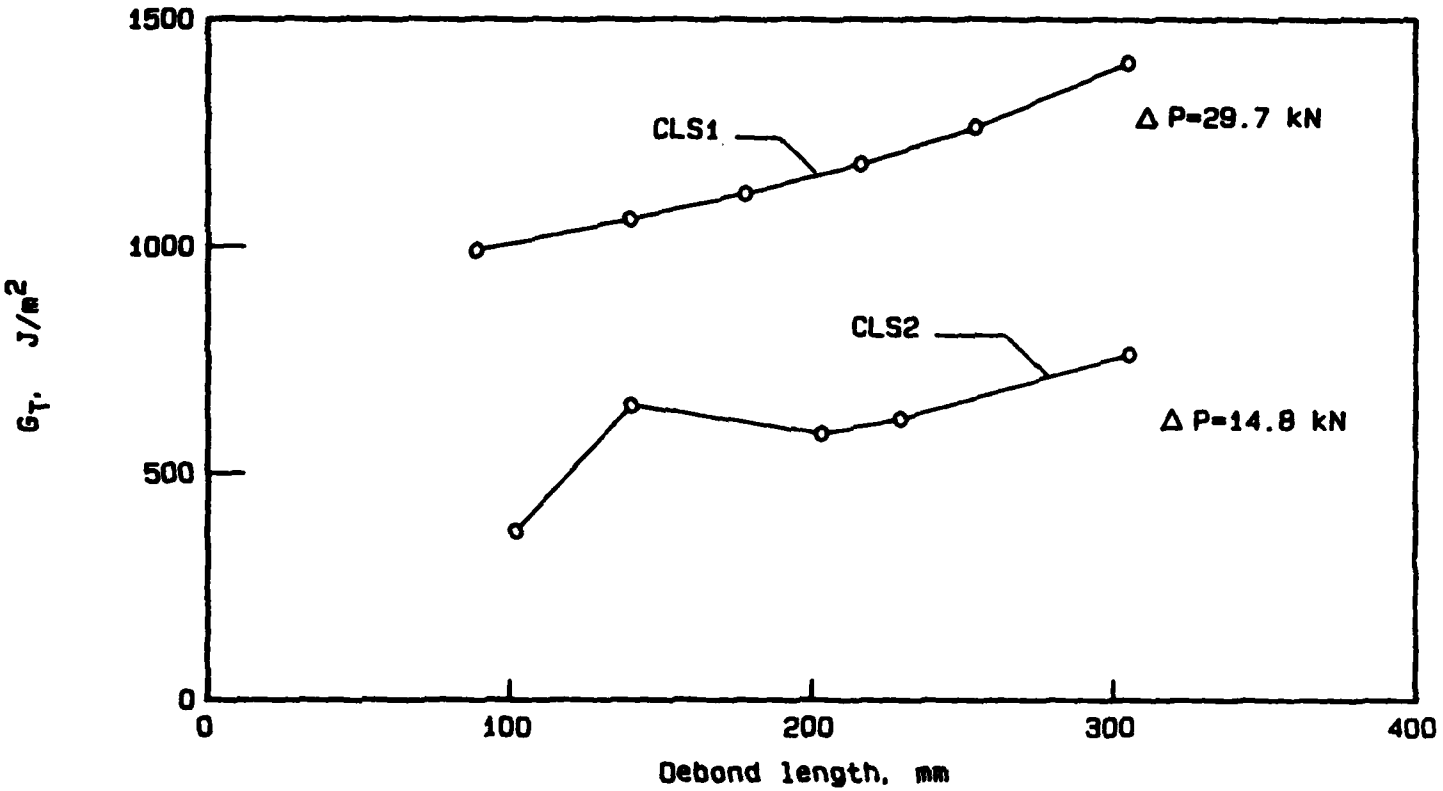

Fig. 6--Variation of strain-energy-release rate with debond length per finite-element analysis.

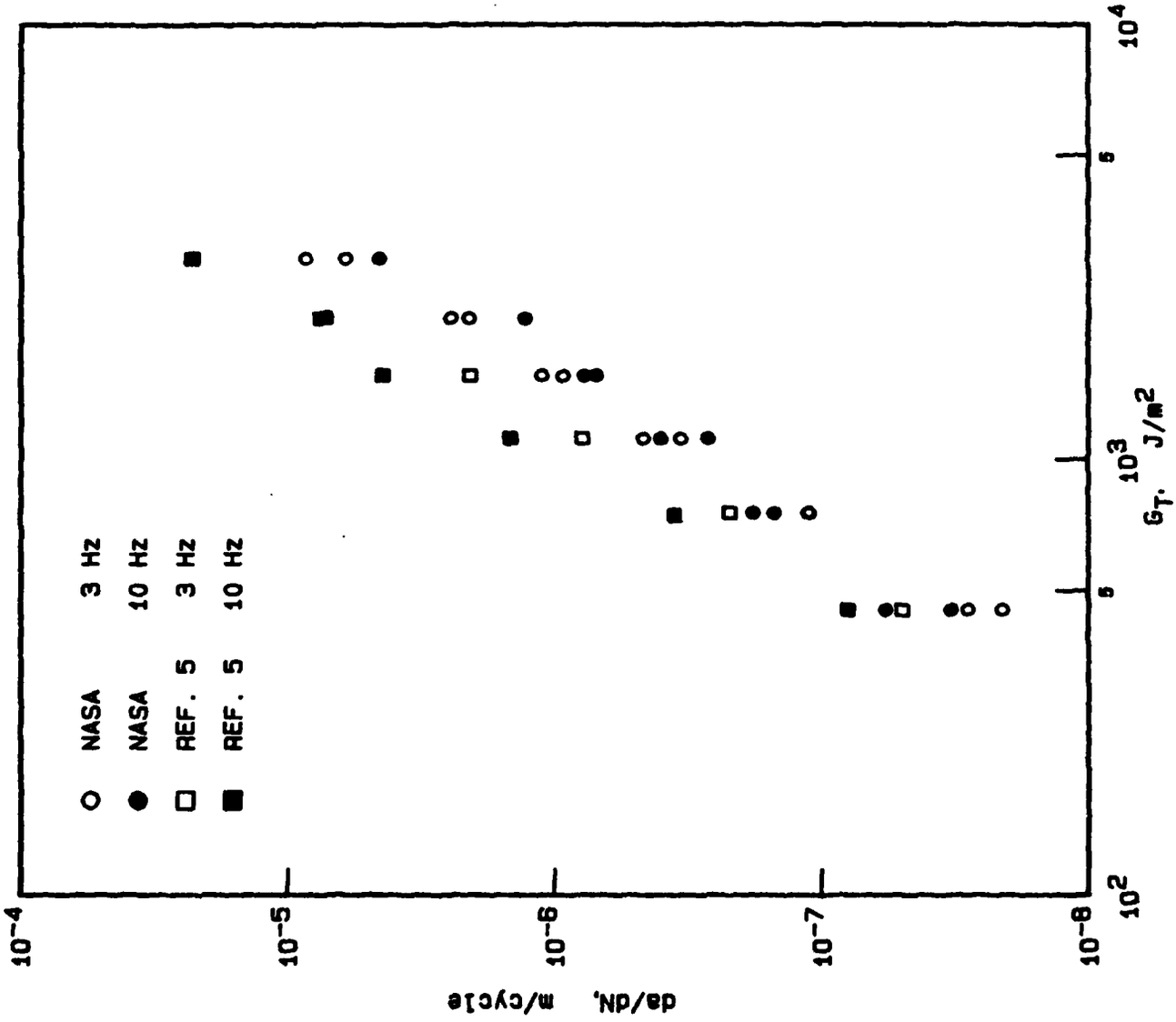

Fig. 7--Debond growth rate for CLS 1 specimens.

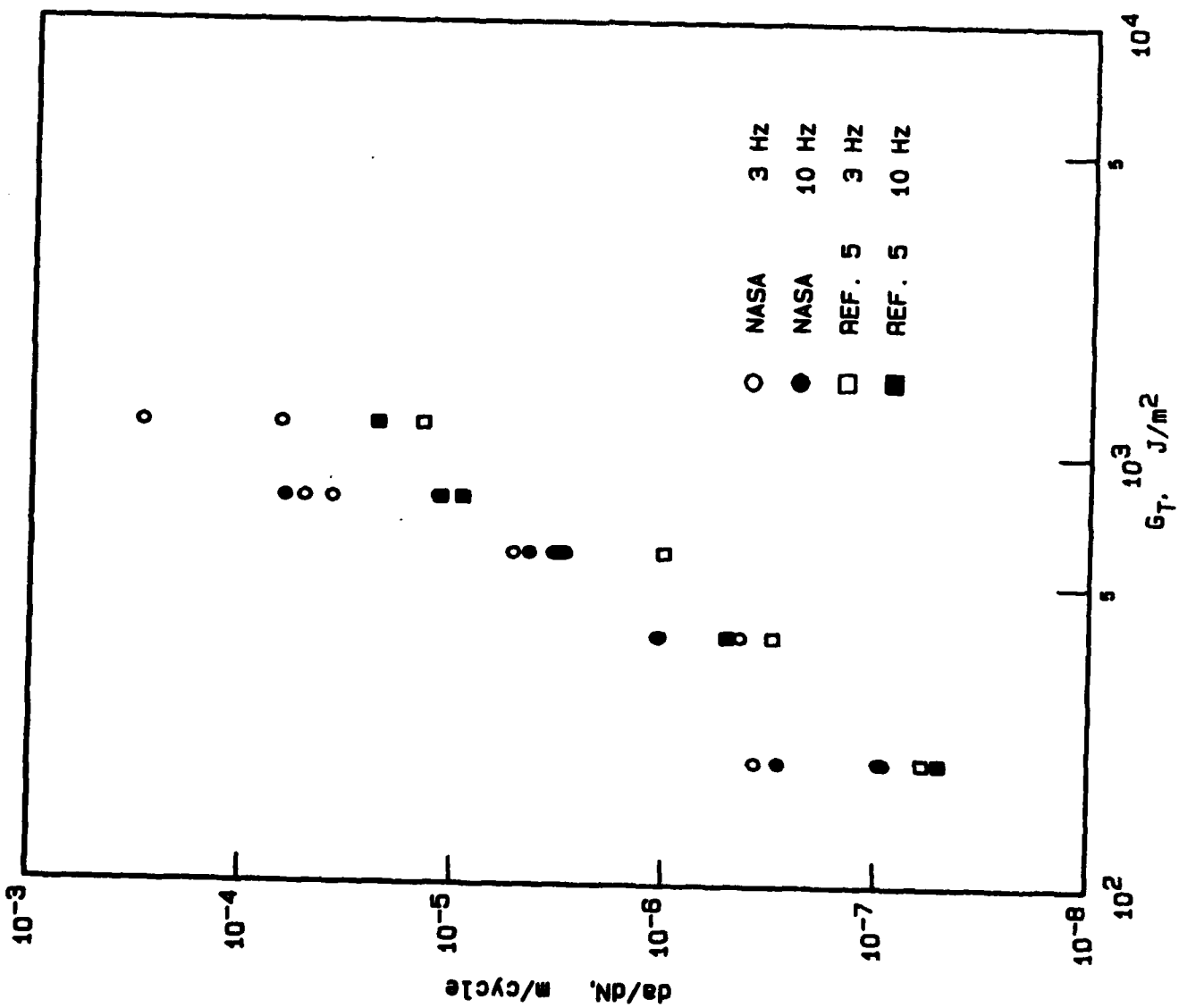

Fig. 8--Debond growth rate data for CLS2 specimens.

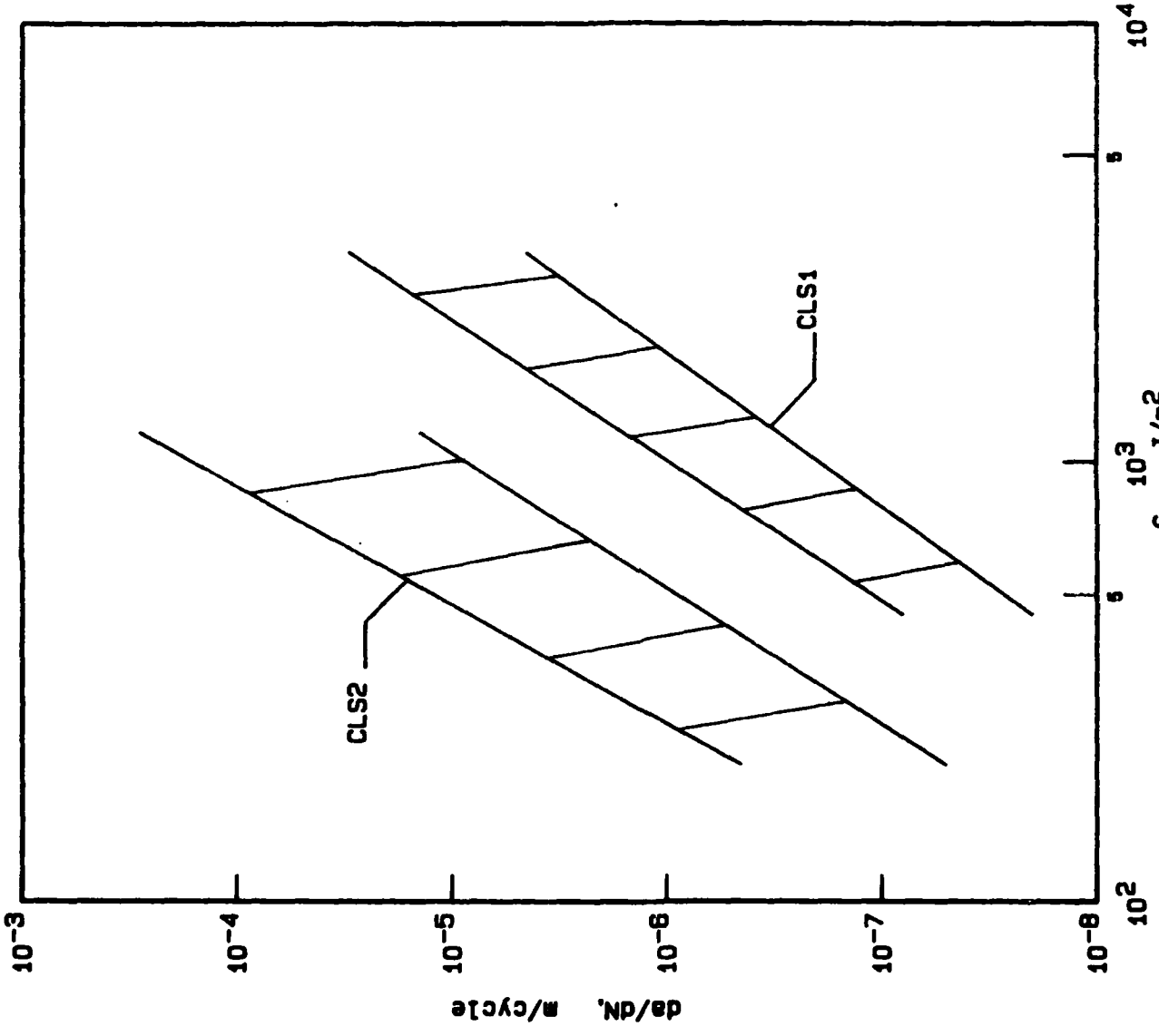

Fig. 9--Comparison of CLS1 and CLS2 debond growth rate data.

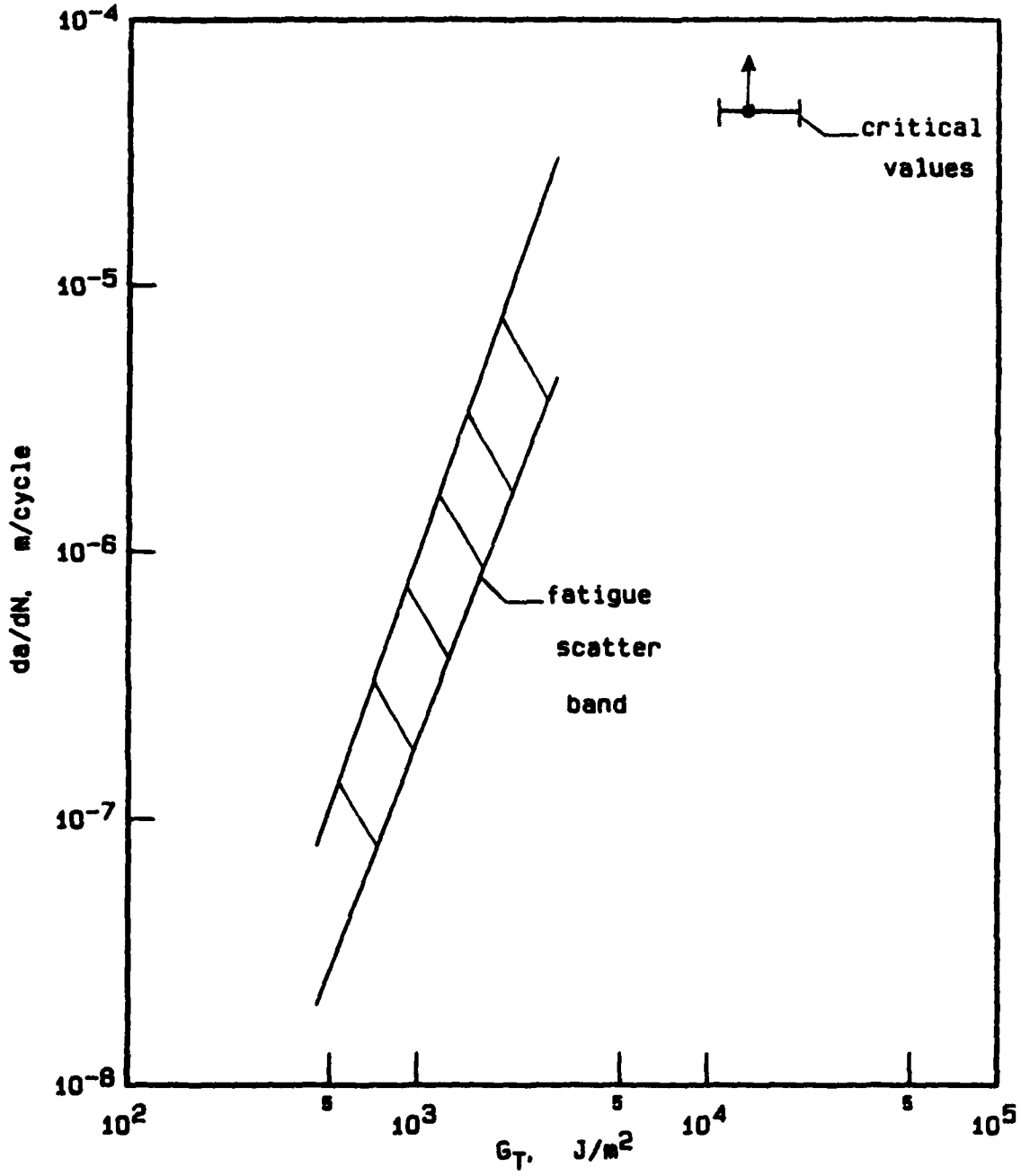

Fig. 10--Comparison of static and cyclic strain-energy-release rate for CLS1 specimens.

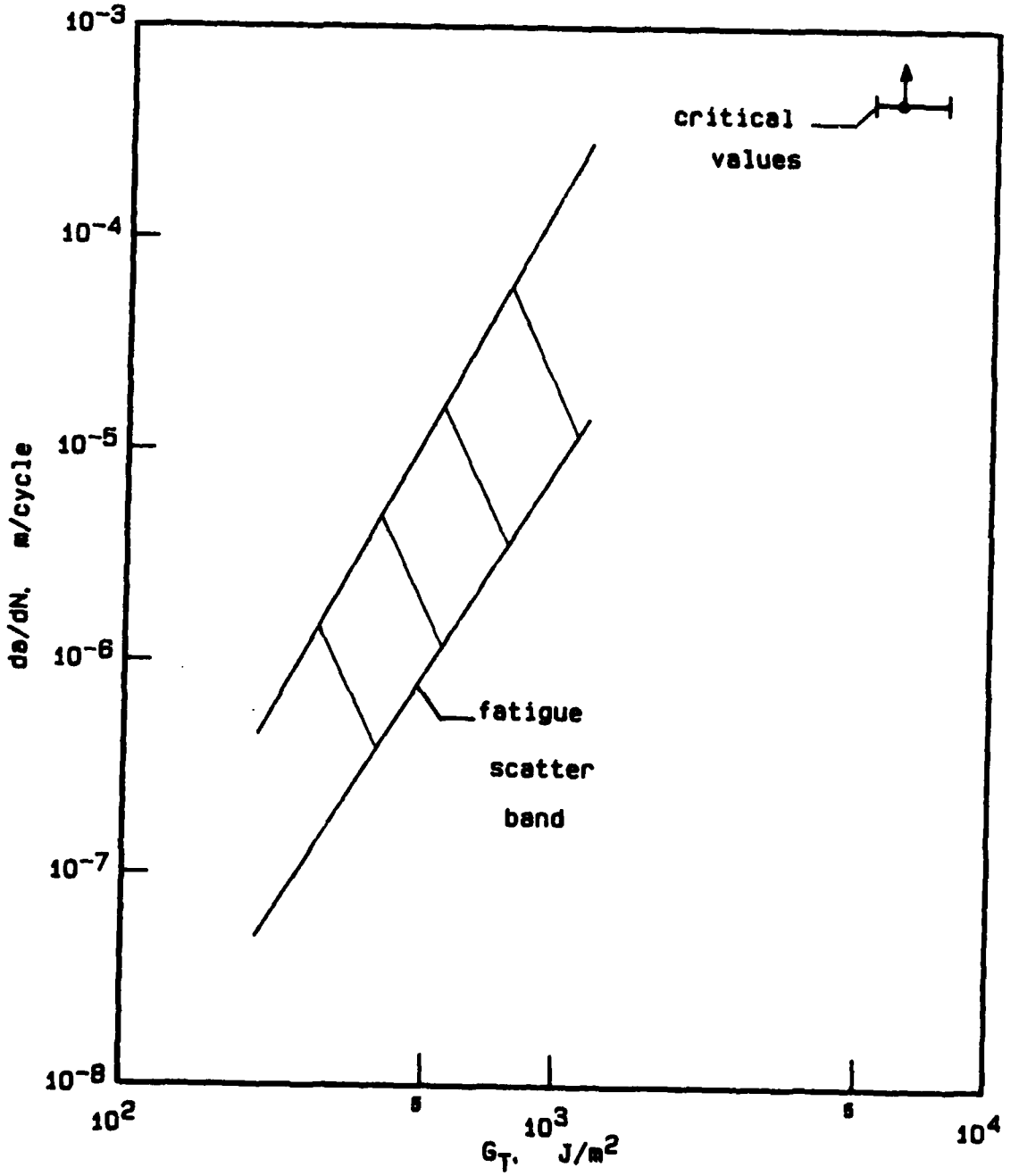

Fig. 11--Comparison of static and cyclic strain-energy-release rate for CLS2 specimens.

1. Report No.	2. Government Accession No.	3. Recipient's Catalog No.
NASA TM-85753, USAAVSCOM TR-84-B-1	AD-A139 809	

4. Title and Subtitle	5. Report Date
REPEATABILITY OF MIXED-MODE ADHESIVE DEBONDING	February 1984
	6. Performing Organization Code: 505-33-33-05

7. Author(s)	8. Performing Organization Report No.
R. A. Everett, Jr.* and W. S. Johnson	
	10. Work Unit No.

9. Performing Organization Name and Address	11. Contract or Grant No.
NASA Langley Research Center, Hampton, VA 23665 Structures Laboratory, U.S. Army Research and Technology Laboratories (AVSCOM), Hampton, VA 23665	

12. Sponsoring Agency Name and Address	13. Type of Report and Period Covered
National Aeronautics and Space Administration Washington, DC 20546 and U.S. Army Aviation Systems Command St. Louis, MO 63166	Technical Memorandum
	14. Army Project No.: 1L161102AH45

15. Supplementary Notes *R. A. Everett, Jr., Structures Laboratory, U.S. Army Research and Technology Laboratories (AVSCOM), Hampton, VA 23665.
This paper was presented at the ASTM Symposium on Delamination and Debonding of Materials, Pittsburgh, Pennsylvania, November 8-10, 1983.

16. Abstract

An experimental study was undertaken to assess the repeatability of debond growth rates in adhesively bonded joints subjected to constant-amplitude cyclic loading. This was done by comparing debond growth rates from two sets of cracked-lap-shear specimens that were fabricated by two different manufacturers and tested in different laboratories. The fabrication method and testing procedure were identical for both sets of specimens. The specimens consisted of aluminum adherends bonded with FM-73 adhesive. Critical values of strain-energy-release rate were also determined from specimens that were monotonically loaded to failure. The test results showed that the debond growth rates for the two sets of specimens were within a scatter band which is similar to that observed in fatigue crack growth in metals. Cyclic debonding occurred at strain-energy-release rates that were more than an order of magnitude less than the critical strain-energy-release rate in static tests.

17. Key Words (Suggested by Author(s))	18. Distribution Statement
Fatigue Adhesive Cyclic debonding Strain energy Repeatability	Unclassified - Unlimited Subject Category 27

19. Security Classif. (of this report)	20. Security Classif. (of this page)	21. No. of Pages	22. Price*
Unclassified	Unclassified	26	A03

*For sale by the National Technical Information Service, Springfield, Virginia 22161